METHANE DETECTION IN THE LOWER TROPOSPHERE RELATED TO THE BURNING OF BIOMASS AND LEAKAGE IN A PETROCHEMICAL POLE, USING RAMAN LIDAR TECHNIQUE

DETECÇÃO DE METANO EM BAIXA TROPOSFERA RELACIONADA À QUEIMA DE BIOMASSA E GASES FUGITIVOS EM PÓLO PETROQUÍMICO, UTILIZANDO A TÉCNICA DE RAMAN LIDAR

Fernanda de Mendonça Macedo[1]; Thaís Correa[1]; Elaine Cristina Araújo[1]; Izabel da Silva Andrade[1]; Roberto Guardani[2]; Igor Veselovskii[3]; Eduardo Landulfo[1]

Artigo recebido em: 16/10/2020 e aceito para publicação em: 22/12/2020.
DOI: http:/dx.doi.org/10.14295/holos.v21i1.12425

Abstract: Fugitive emissions, defined as unintended or irregular leaks of gases and vapors, are an important source of pollutants to the atmosphere, which is difficult to monitor and control. These sources are present in different sites, especially in regions that are growing in size and economic activity. In this study, we present the results of the capability to detect methane profiles at low troposphere combining data retrieval correlations between a rotacional/vibracional Raman lidar (RVRL) and a cavity ring-down spectrometer (CRDS). The measurements were made at two different sites, metropolitan area of São Paulo (MSP) and industrial area of Cubatão (IC). The lidar is based on a tripled Nd:YAG laser with a 20 Hz repetition rate, operating on the 355 nm wavelength elastic channel, the 353 nm and 396 nm wavelength inelastic channels. A measurement protocol was established, considering acquisition time for signal accumulation, climatic conditions and data above and below the planetary boundary layer. The idea was to establish specific measurement procedures for situations related to product leakage in the oil process and natural events, such as biomass burning. With over 150 hours of data acquisition, the results pointed the possibility of analyzing data from distances up to 1500 m with an initial resolution of 7.5 m which was extended to 100 - 300 m after data smoothing for obtaining final results. The concentration was calculated from the ratio between the methane Raman backscatter signal and the nitrogen signal, at 396 nm and 353 nm, respectively. The temporal variation of methane concentrations was correlated with CRDS data, in order to obtain a first degree calibration.

Keywords: Lidar. Raman. Methane. Remote Sensing. Greenhouse gases.

Resumo: As emissões fugitivas, definidas como vazamentos não intencionais ou irregulares de gases e vapores, são uma importante fonte de poluentes para a atmosfera, de difícil monitoramento e controle. Essas fontes estão presentes em diferentes locais, especialmente em regiões que estão crescendo em tamanho e atividade econômica. Neste estudo, apresentamos os resultados da capacidade de detectar perfis de metano na baixa troposfera combinando correlações de recuperação de dados entre um Raman lidar rotacional / vibracional (RVRL) e um espectrômetro de cavidade ressonante (CRDS). As medidas foram realizadas nas regiões metropolitanas de São Paulo (RMSP) e Cubatão. O lidar é baseado em um laser Nd: YAG triplo com uma taxa de repetição de 20 Hz, operando no canal elástico de comprimento de onda de 355 nm e em canais

[1] Instituto de Pesquisas Energéticas e Nucleares (IPEN). E-mail: (fernanda.macedo@fatecpg.com.br, correa-thais@hotmail.com, elaine.c.araujo13@gmail.com, izaabel94@hotmail.com, landulfo@gmail.com)
[2] Universidade de São Paulo (USP), São Paulo, SP. E-mail: (guardani@usp.br)
[3] A.M. Prokhorov General Physics Institute, Moscow. E-mail: (iveselov@hotmail.com)

inelásticos de comprimento de onda de 353 nm e 396 nm. Um protocolo de medida foi estabelecido, considerando o tempo de aquisição para o acúmulo do sinal, as condições climáticas e os dados acima e abaixo da camada limite planetária. A ideia era estabelecer procedimentos de medidas específicas para situações relacionadas a vazamento de produtos no processo de óleo cru e eventos naturais, como a queima de biomassa. Com mais de 150 horas de aquisição de dados, os resultados apontaram a possibilidade de análise em distâncias de até 1500 m com resolução inicial de 7,5 m que foi ampliada para 100 - 300 m após suavização dos dados para obtenção dos resultados finais. A concentração foi calculada a partir da razão entre o sinal de retroespalhamento Raman do metano e o sinal do nitrogênio, a 396 nm e 353 nm, respectivamente. A variação temporal das concentrações de metano foi correlacionada com os dados do CRDS, a fim de obter uma calibração de primeiro grau.

Palavras-chave: Lidar. Raman. Metano. Sensoriamento remote. Gases de efeito estufa.

1 INTRODUCTION

Methane (CH_4) is one of the most important greenhouse gases and can be released into the atmosphere from both anthropogenic sources such as the energy sector (coal and gas extraction), the agricultural sector (rice fields, animals) and natural sources (wetlands and forest fires) (KAVITHA, 2016, BARAY, 2018). As an active participant in the chemistry of tropospheric air pollution, it plays an important role in the Earth's radiative balance and there are obvious concerns about the impact of CH_4 on the atmosphere, leading to an increase in global temperature related to these different emission sources (IPCC-AR5, 2014). It is known that the concentration of basal methane from natural sources is 2 about ppm, however if it is quantified within the planetary boundary layer, this value can more than double due to emission sources (BARAY, 2018). Fugitive gases are one of the major pollution sources and at the same time of difficult monitoring and control (WEINBRING, 1998). In 2015, in Brazil, oil and natural gas emissions accounted for 87% of greenhouse gas emissions from fugitive subsectors (Berndt, 2018). The CH_4 emission, as a fugitive gas, from extraction, processing and transportation of oil and natural gas facilities, was 170.9 Gg of CH_4 (BERNDT, 2018).

Considering a refinery site, gaseous plumes emanating from individual process sources are often intermittent at low concentrations and make it difficult to monitor possible fugitive gases, therefore, a sensitive and remote system for low concentrations is required. Another possible source of methane emission that requires intense study and great attention is the forest fire, which is an important and persistent threat to the environment, human health and economic development. In Brazil, more than 300,000 fires are detected per year and this number has been increasing. Forest fires cover large areas in Brazil, where about 85% occur in the territory of the Legal Amazon.

The practice of burning is common as part of pest control in agriculture, clearing of planting areas, pasture renewal and sugarcane harvesting. Generally, biomass burning is the most serious source of gases, combining greenhouse gases such as methane (CH_4). Megacities and industrial sites, are growing in size and economic activity (FREJAFON, 1998), at the same time, there is a remarkable growth in concerns about the environmental issues associated with these activities. Among the necessary information to be provided to mitigate the environmental and health consequences of economic activities is the necessary reliable and real-time information on air pollutant emission rates. This information is an essential tool for industries and environmental authorities. Remote laser sensing techniques such as lidar, can provide a real-time information and transfer reliable data on fugitive emissions. This non-intrusive technique is capable of providing data from distant locations with high spatial resolution. For the high measurement of Raman transverse dispersion, high concentrations of the studied atmospheric components are indispensable, therefore nitrogen is a reference gas because its atmospheric concentration is well known and widely studied (WEBER, 1979).

This study used the vibrational-rotational Raman lidar, being a powerful tool for identification and quantification small fractions in complex mixtures, even considering the symmetrical structure of nitrogen and methane molecules, since the spectra are well organized and understood (EISBERG, 1985). The principle of Raman scattering is that the incidence energy of an atmospheric molecule may alter its quantum state and the frequency of the scattered photon is changed. Raman Stokes is one of the processes, that occurs when the molecule transfers a photon energy scattered, by decreasing it´s energy level, increasing the frequency of the scattered photon.

According to Weber (1979) methane acts on a Stokes process, when excited with the wavelength 355 nm, changing the Raman frequency to 396 nm. This result may be confirmed when their scattering cross sections are normalized to the cross section of nitrogen, when excited with a 355 nm wavelength. The vibrational Raman line for methane, 2914 cm^{-1}, is well isolated and has a scattering cross section 8 times greater than nitrogen. The reason why there is a need for signal accumulation and a robust Raman system is because the basal methane concentration is low, about 1800 ppb (WEBER, 1979). Still based on the signal accumulation, Veselovskii (2019) studied statistical uncertainty for vertical profiles, of three values of the aerosol extinction coefficient: 0.05; 0.1; 0.2 km^{-1} and an average signal time of 4 hours.

The photon count rate in methane Raman channel is $v_{CH_4} = N_{CH_4}^{ph} \frac{2\,\Delta z}{c}$ where *c* is the speed of light. For a clean atmosphere (α_{355} = 0.05 km^{-1}) uncertainty in the measurements below 10% are possible up to 4 km, while for (α_{355} = 0.2 km^{-1}), the interval decreases to 3 km away. The simulation results confirm the need for long-term accumulation signal (several hours) in methane measurements using the Raman lidar (VESELOVSKII, 2019). In order to correlate optical data, we decided to use Cavity ring-down laser spectroscopy (CRDS), which is one of the techniques developed to monitor fugitive gases in the atmosphere. However, despite the high accuracy in the detection of low levels of pollutant gases in the atmosphere and the relative decrease in the cost of detectors, this technique is not able to provide spatial resolution of the amount and dispersion of these gases, but helped in the methane gas quantification during the campaigns carried out. Throughout this study, several sensitivity tests were performed to investigate and understand the signal behavior when measuring methane-nitrogen ratios according to literary exposure. Based on these premises, a routine was developed for a data acquisition protocol.

This paper presents the results of the vertical profile of methane in a megacity with intrusion of natural emissions, biomass burning emissions and fugitive gas emissions from the oil refining process.

2 MATERIAL AND METHOD

The low intensity of the Raman backscatter signals requires a specific configuration of the lidar technique, requiring a high-power laser transmitter and a highly efficient reception and detection system. The lidar is based on a tripled Nd:YAG laser with a 20 Hz repetition rate, and a pulse energy of 70 mJ at 355 nm. A 30 cm aperture Newtonian telescope, collects the backscattered light. The optical signal is delivered to the detection module by means of an optical fiber. The lidar contains a separate detection module with a three - channel module (TCM) for detection of elastic backscatter at 355 nm, rotational Raman backscatter at 353.9 nm and methane vibrational Raman scattering at 394 nm. The optical fiber can be switched between the detection modules for specific tasks. The optical signal from the fiber is collimated in the TCM by a silica lens and the collimated beam is separated for the spectral components by two dichroic mirrors.

The spectral components are isolated by the interference filters and detected by R9880 PMTs. The outputs of the detectors are recorded at 7.5 m range resolution using

Licel transient recorders that incorporate both analog and photon-counting electronics. The full geometrical overlap of the laser beam and the telescope field of view (FOV) is achieved at approximately 500 m height for 1.0 mrad the field of view used. The TCM allows both Mie - Raman aerosol and Raman methane measurements. The interference filter (Alluxa, CA, USA) centered at 393.9 nm of 1 nm FWHM selects the group of rotational Raman lines of oxygen and nitrogen near the isosbestic point, to minimize the temperature dependence of efficient scattering cross section (INABA, 1976) The use of rotational Raman scattering allows to increase the backscattered power to more than factor 10 comparing to vibrational Raman nitrogen component at 387 nm. Moreover, separation of 353/397 nm wavelengths by dichroic mirror is easier than 387/397 nm. Suppression of 354.7 nm elastic scattering by rotational Raman filter is above 10^4, so two normally installed interference filters were used together to provide more than 8 orders of magnitude of rejection of the elastic signal. The interference filter (Alluxa, CA, USA) in the methane Raman channel was centered at 395.7 nm.

The filter bandwidth was 0.3 nm and the peak transmission was above 80%. Suppression of 355 nm radiation was specified by the manufacturer to be above 12 orders. Due to the low methane Raman backscatter the measurements were performed at night time only. With the support of a digital phosphor Oscilloscope (Tektronix, TDS 580D), it was possible to certify that the photo-multipliers signal intensity was adequate for the measurements to be performed. In the elastic backscatter technique, the backscatter coefficients and extinguishing aerosol should be determined from a single measured signal. The inelastic backscatter signal is affected only by the aerosol extinction term, but not for its backscatter (ANSMANN, 1992). As Veselovskii (2019), the equation below describes the procedure for evaluating methane acquisition data for Raman measurements.

$$N_x^{ph}(z) = O(z)A_x \frac{E}{hv}\Delta z \frac{S}{z^2}\, N_x\sigma_x\, exp\left\{-\int_0^z (\alpha_L^a + \alpha_L^m + \alpha_x^a + \alpha_x^m)\, dz'\right\}$$

In which, $O(z)$ is the geometrical overlap factor, A_x is an efficiency factor, including the transmission of the optics and the quantum efficiency of the detectors. E and hv are the laser pulse and the photon energies, Δz range resolution, S receiving telescope area, N_x number concentration and α is the extinction coefficient, where superscripts "a" and "m" indicate aerosol and molecular contributions, respectively. Subscripts "L" and "x" correspond to the laser wavelength λ_L and to the wavelength of Raman backscatterλ_x. The factor

$n_x X \frac{\sigma_x}{\sigma_{N_2}}$ is necessary for a good performance during the detection of the molecule x (where n_x is the mixing ratio of the molecule "x"), which is approximately 10^4 for the H_2O molecule and about 320 for CO_2. Considering CH_4 as the main gas of interest in this work, this factor is about 20 times less than that of CO_2, requiring a powerful Raman to deal with a high signal accumulation time. The methane / nitrogen mixture ratio can be calculated from the ratio of its Raman lidar signals (P_{CH_4} and P_{N_2}), corrected for the extinction of the aerosol and the molecular differential (2019):

$$n_{CH_4}(z) = k \frac{P_{CH_4}}{P_{N_2}} \exp\left\{ - \int_0^z \left[\alpha_{N_2}^a \left(1 - \left(\frac{\lambda_{CH_4}}{\lambda_{N_2}} \right)^{-\gamma} \right) + \alpha_{N_2}^m \left(1 - \left(\frac{\lambda_{CH_4}}{\lambda_{N_2}} \right)^{-4} \right) \right] dz \right\}$$

Here $\lambda_{N_2}$and λ_{CH_4} are the wavelengths of nitrogen and methane Raman components; $\lambda_{N_2}^a$ and $\lambda_{N_2}^m$ are the aerosol and molecular extinctions at λ_{N_2} ; γ is the Ångstrom exponent and k is the calibration constant. For calibration purposes, in our measurements, we assume that the CH4 mixing ratio above the boundary layer is 2 ppm (BARAY, 2018).

In order to compare and determine the molar ratio of the CH_4 and N_2, the CRDS technique was used, where the optical absorption analysis of atoms, molecules and optical components is performed (O´KEEFE, 2009).

The CRDS configuration, measures how long it takes the light to reach $1/e$ of its initial intensity and this "touch time" can be used to calculate the absorbent CH_4 concentration of the gas mixture inserted in the cavity.

Assuming that the switching time of the Pockels cell is short in relation to the cavity decay time, the measured cavity output decays exponentially according to the expression:

$$I(t) = I_0 \times exp^{(-t/\tau)}$$

Where τ is the cavity deterioration time constant.

In the case of a cell with an effective path length of several kilometers, the resonant light trapped between the mirrors leaks over a relatively long time scale, ~ 3 μs.km^{-1}. The intensity of the light that leaves the cell can described as single exponential (LEHMANN, 1996):

$$I(t) = I(0)\ exp\left[\frac{-tc}{L}\ (1 - R + \varepsilon CL)\right] = I(0)exp\left[\frac{-t}{\tau}\right]$$

where $I(t)$ is the time-dependent light intensity leaving the cavity; $I(0)$ is the initial light intensity; c is the speed of light in the medium between the mirrors; C is the concentration of the absorbing species; L is the separation between the mirrors; and t is the decay time constant of the cavity, or "ring-down" time, defined as the amount of time it takes for the intensity to reach $^1/_e$ of the initial intensity.

2.1 Procedures

Throughout this study, the lidar sensitivity was tested to assimilate the interaction and the behavior of the inelastic signal (353 nm and 396 nm) towards the N_2 and CH_4 molecules, as well as the elastic signal (355 nm). The first step was to attempt for the optical geometric arrangement between the sending and receiving systems, which determine the degree of signal compression (WEITKAMP, 2005). Taking into account that this study was carried out with a biaxial lidar, where the optical axes are spatially separated, only part of the backscattered signal is measured.

To make this minimized, improving the entry of the optical path in the telescope's field of view, it was necessary to align the system making the overlap function, for adjacent distances, as close as possible to the receiver's field of view. Using an oscilloscope, adjustment was made between amplitude and frequency in order to indicate a good overlap function.

The second important step was to evaluate the electronic behavior of the detection system, measuring the dark current (DC). After completely covering the telescope and the optical detection box with black cloth, in order to prevent any radiation from reaching the detection system, the system was put into operation and the response of the PMTs (photomultiplier) and APD (Avalanche PhotoDiodes) was monitored during the period of 10 minutes. In order to perform the DC test, it was also necessary that all measurement parameters, such as the voltage applied to the detectors, repetition frequency and laser power, were configured under normal measurement conditions (GUERRERO-RASCADO, 2014). The third step is to decide the signal stability related to the number of shots. It is important to determine the number of shots that the transient recorder accumulates to

generate a file with the average of the accumulated signals. For each shot, a complete measurement of the atmospheric profile is performed along the optical laser path.

The greater number of laser shots, the greater integration interval and more measurements are taken in a single profile, generating greater stability of the signal in this file. The fourth stage is linked to the ideal angulation and the planetary boundary layer of the region under study. In MSP, which has a more stable planetary boundary layer, and we can also observe a lot of atmospheric transport, we were able to use a higher angle. In the case of IC, where the planetary boundary layer is unstable and the topography is irregular with the Mata Atlântica forest very close to the measurement site, smaller angles were used. In this case, the aim was to acquire fugitive gas data from oil processing, which also led to a lower angle. Meteorology is also an important factor since the system cannot operate with rain, fog and low cloud cover.

3 RESULTS

The measurements were carried out in the campus of the University of São Paulo, at the laboratories of the Institute of Energy and Nuclear Research (IPEN), and Environmental Research Centre (CEPEMA), with clear sky.

In total, more than 90 sessions of night analysis were performed, for a better temporal resolution, a long signal accumulation time was required, which was about 8 hours (2018).

The measurements campaigns were accompanied by a Cavity Ringdown Laser Spectroscopy (CRDS) system, a greenhouse gas analyzer, Los Gatos. This system was chosen for primary characterization of CH_4 in both sites acquisition. It was chosen because of its sensitivity and small stability.

When relating height and distance to the target molecule studied, the relationship between the optical path and the ground must be observed.

For this study, an optimized inclination angle was chosen for field measurement carried out at IPEN anda CEPEMA, with respect to the angular elevation so that the optical path as close as possible the sources of methane leakage. The detection sensitivity and the adjustments of the specific parameters of the system, such as voltage of the PMTs related to the signal gain, repetition rate, integration time of each sampling, temperature, speed and wind direction were also considered.

Table 1 shows the conditions adopted in the campaign carried out on April 3 and 4, 2019, at the IPEN site. The results refer to the an accumulated time of 10 hours.

Table 1 - Detection limits and acquisition strategy for April 3rd, 2019 measurement.

Date	04/03/2019
Local	IPEN –SP 23°33'59.10"S ; 46°44'16.80"
Acquisition period	06 h:30 pm – 04 h:30 am
Wind direction	Northeast
Inclination	54º
Integration time (min)	30 - 60
Voltage (V)	353 nm - 790 355 nm - 700 394 nm - 910
Repetition rate (Hz)	20
# Shots	2000
Average surface temperature (ºC)	22.8
Surface wind speed (m/s)	1.0
Detection limit (ppm)	2 - 3
Detection time (s)	60
Resolution (m)	7.5 (30 – 100)
Detection range (Km)	~1.0

The results are shown in figure 1, the Raman system was able to detect a natural episode, in an average proportion which enhance the Raman signal almost to the double of the baseline. This event was a fire, which occurred in the forest of the peak of Jaraguá in São Paulo, located at approximately 10 km from the acquisition site.

We see an emission pattern in the red and orange lines, which are related to the beginning of the acquisition period and the intermediary period.

When analyzing the final period (blue and gray lines) we noticed a slight increase in distance of 400 m from the point of analysis of the data and then a fall. According to local media, the fire started at 8 pm and the fire started to be controlled around midnight. This fact shows evidence of the relationship with the drop in the Raman signal.

The data analysis indicates an intense plume of aerosols entering the atmosphere between 1000 m and 1500 m altitude and at the same time close to the surface below 500 m. As it is a fact related to the burning of biomass, the atmosphere had an increase in aerossol.

A CRDS analysis indicates a high concentration of CH_4, which reached double the standard value, 4 ppm (Figure 2), during the acquisition period. This fact is confirmed with the data presented in Figures 1 A and 1 B, where an increase of CH4 concentration is observed.

Figure 1 - Vertical profile of CH_4 mixing ratio Raman signal, along distance (A) and height (B) on April 3rd, at the IPEN analysis site

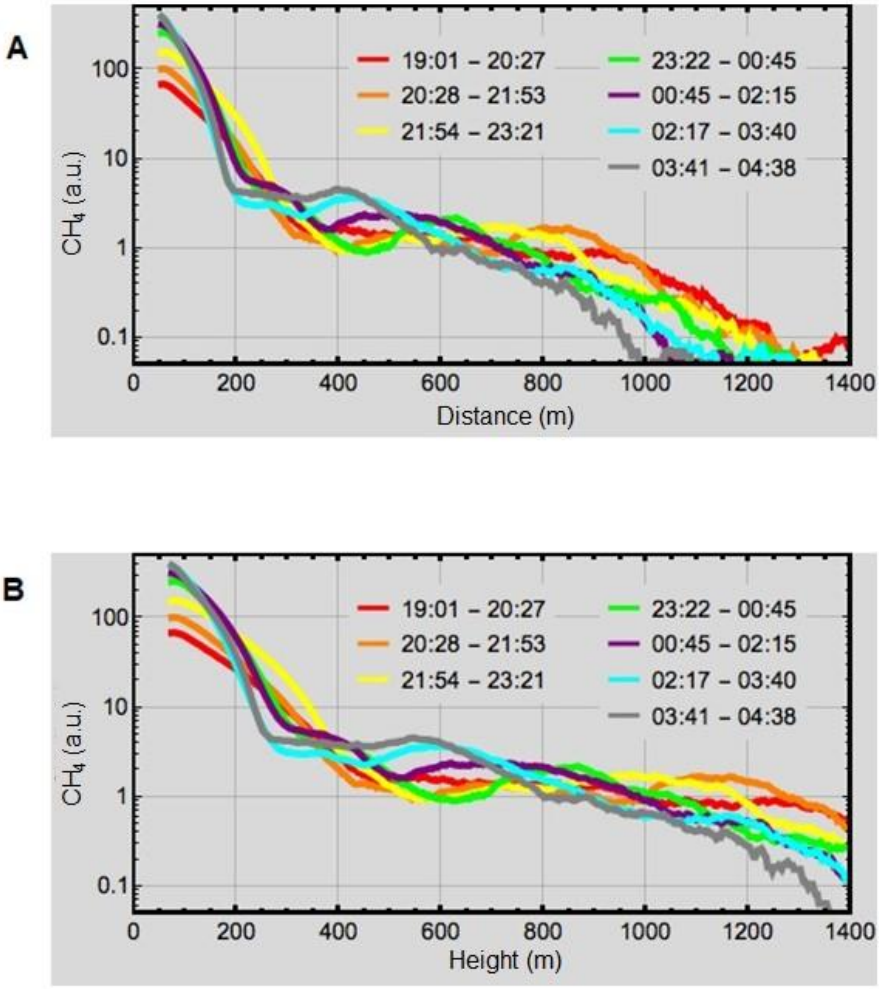

Generally, burning biomass is the most serious source of gases, combining greenhouse gases, such as methane (CH_4). According to Tihay-Felicelli (2017), the contribution of CH_4 as a greenhouse gas is 62 times greater than CO_2 when analyzed during the burning phases (propagation phase, flaming combustion and slow combustion). An important fact occurs in the combustion and slow combustion phases, CH_4 can be released in the two mentioned phases. In the first, a rich mixture of air-degrading gases may prevail, incomplete combustion, inducing CH_4 production. Slow combustion is a solid phase reaction and has a lower O_2 exchange, induces a heat release rate that modifies normal combustion, producing incomplete combustion and generating CH_4 emission. In Figures 1 A and 1 B we noticed that the increase in the Raman signal, as well as an increase in the concentration of the methane fraction occurred after the control of the forest fire, that is, in the phase of slow combustion (latent heat).

Figure 2 - Quantification of CH_4 concentration in ppm, by CRDS, on 04/03/2019, at IPEN site, where the red line indicates the moving average for this period

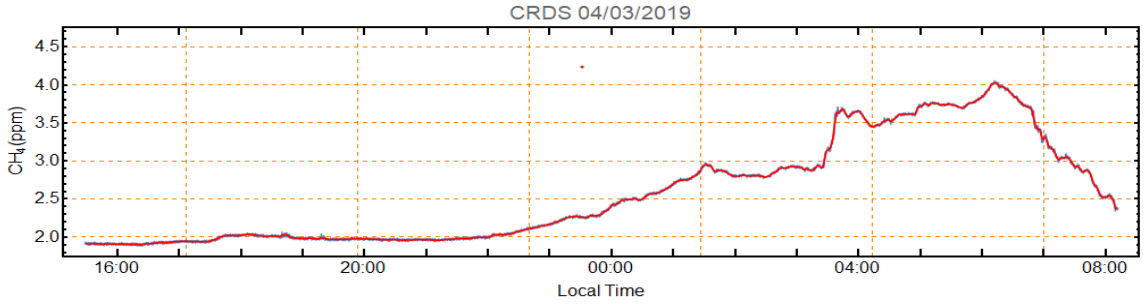

During December 2019 and January 2020, a total of more than 60.0 hours of sessions in site acquisitions, was performed during night period, at CEPEMA, in Cubatão. The lidar system was positioned towards the flare of an oil refinary, aimed at the capture of possible process fugitive gases. Table 2 shows the conditions adopted in the campaign on January 10, 2020.

Figure 3 shows the profile of CH_4 Raman signal obtained on this acquisition date. The signals were integrated approximately 1 h and 30 min, with measurements of height (Figure 3 A) and distance (Figure 3 B). When analyzing the Raman signal for this acquisition period, we found an elevation profile of CH_4 signal practically throughout the period, highlighting the last period (green line) where the signal seems more frequent and intense throughout. When analyzing the signal during the last three periods, we observed, in addition to the frequency, an increase in the elevation of that signal.

The CH_4 mixing ratio, in arbitrary units for Raman signal, related to the same data shown in the previous figure, becomes clear that there is a frequent emission of CH_4 over the acquisition period, and that it becomes more intense after 600 m.

Table 2 - Detection limits and acquisition strategy for January 10th, 2019 measurement

Date	01/10/2020
Local	CEPEMA –SP 23°53'11.00"S ; 46°26'16.30"W
Acquisition period	22:00 pm – 05:00 am
Wind direction	Northeast
Inclination	21º
Integration time (min)	30 - 60
Voltage (V)	353 nm - 640 355 nm - 700 394 nm - 800
Repetition rate (Hz)	20
# Shots	1200
Average surface temperature (ºC)	35.7
Surface wind speed (m/s)	1.3
Detection limit (ppm)	2 - 3
Detection time (s)	60
Resolution (m)	7.5 (30 – 100)
Detection range (Km)	~1.0

Figure 3 - Vertical profile of CH_4 mixing ratio Raman sinal, between distance (A) and height (B) on January 10th, 2020, at the CEPEMA analysis site

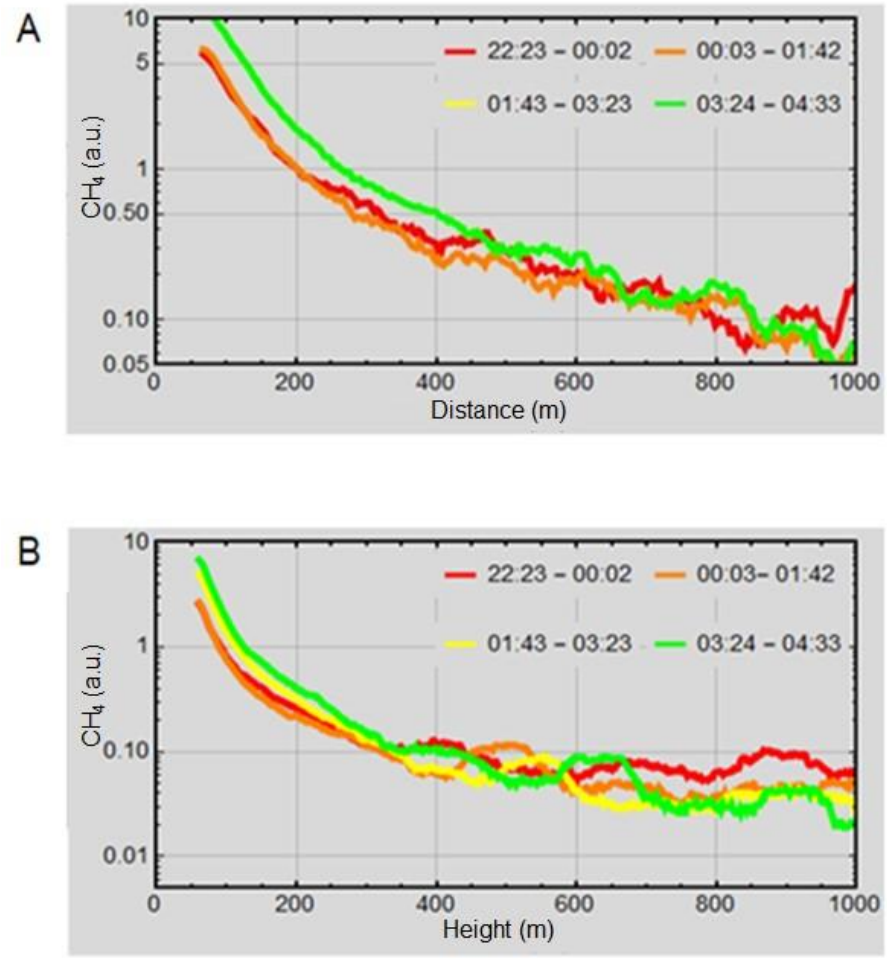

The CRDS analysis for the same period, makes clear what was evidenced in the analyzes in the figures 3 A and 3 B. The frequency and the increase in Raman signal are related to the increase in the concentration up to 3.5 ppm of CH_4 (Figure 4), at CEPEMA site. This indicates that a significant emission of methane took place during the measurement period.

Figure 4 - CH_4 quantification in ppm, on 01/10/2020, at CEPEMA analysis site, where the red line indicates the moving average for this period

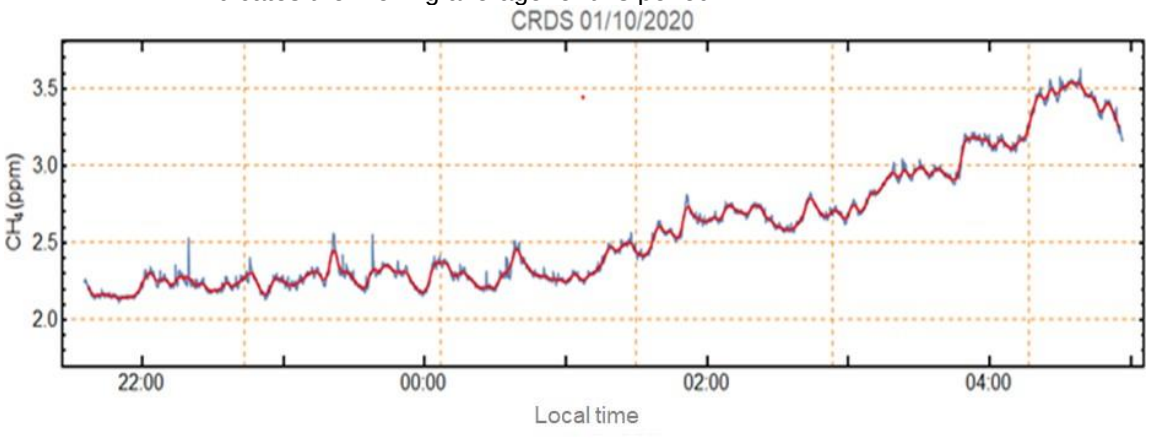

In this case, the change to a lower inclination angle resulted in an approximation of the optical path to a possible source of fugitive CH_4 emission, coming from the oil processing plant or some industrial effluent treatment station, inside the processing site. As mentioned in Rahimpour (2012), the flares of oil-producing units derived from petroleum should be constantly fed with flare gas, where CH_4 is in its majority composition.

This fact shows evidence that one of the possible factors would be an unintentional leak in the flare gas line, as it is approximately 400 m (FACUNDES, 2011) from the acquisition site. The increase in the ambient temperature on the surface is also an important fact to highlight, as Segers (1998) confirms that the increase in temperature is directly proportional to the methane emission.

4 CONCLUSION

In this study, a protocol for methane acquisition data with a Raman vibrational rotational lidar system was established in different acquisition sites.

As it is a unique equipment in Brazil and the second on a global scale to detect CH_4 by Raman remote sensing, a series of analyses and adjustments were necessary depending on the site of acquisition or possible sources of emission.

We found that the differences in the geographical locations of the possible sources at the acquisition sites can interfere with the elevation degree system. When the emitting source is close to the ground, Like the second case study, where the lines in an oil refining production site, the lowest elevation possible should be used. As in this case it is an involuntary CH_4 leakage, the emission concentration is very low and not easy to detect, If the methane source is too distant (the optical path is high), this fraction can suffer influence

of meteorological conditions, mainly the changes in the wind direction and intensity. These circumstances can dissipate the methane fraction.

This would be the case for methane resulting from the burning of biomass, which is transported at higher altitudes and for a prolonged time, since its emission continues during the latent heat phase.

The importance of having equipment in parallel to quantify methane acquisitions was noted. In this case, the use of CRDS was essential, supporting the measures taken, giving a positive return to the study. It is worth remembering that the CRDS is a self-calibrating equipment, making its use easier.

By linking the development of this work with the continuous improvement of the environment, the Raman vibrational rotational system can assist in the detection of one of the main gases that imply the intensification of greenhouse effect, responsible for maintaining the planet energy balance.

5 ACKNOWLEGMENTS

The authors direct sincere thanks to the RCGI - Research Center on Gas Innovation, IPEN, and CEPEMA - USP for the financial support to the present project

REFERENCES

ANSMANN A., RIEBESSELL M. Measurement of atmospheric aerosol extinction profiles wih a raman lidar. **Opt Lett,** v.15, p. 746–748, 1992. https://doi.org/10.1364/OL.15.000746

BARAY, S.; DARLINGTON, A.; GORDON, M.; HAYDEN, K. L.; LEITHEAD, A.; LI, S.-M.; LIU, P. S. K.; MITTERMEIER, R. L.; MOUSSA, S. G.; O'BRIEN, J.; STAEBLE, R.; WOLDE, M.; WORTHY, D.; MCLAREN, R.. Quantification of methane sources in the Athabasca Oil Sands Region of Alberta by aircraft mass balance. **Atmos. Chem. Phys.,** v. 18, p. 7361–7378, 2018. https://doi.org/10.5194/acp-18-7361-2018

BERNDT, A. et al. **Estimativas anuais de emissões de gases de efeito estufa no Brasil**. 4. ed. Ministério da ciência, tecnologia, inovações e comunicações. 2018.

EISBERG, R.; RESNICK, R. **Quantum physics of of atoms, molecules, solids, nuclei, and particles**. 2nd ed. John Wiley & Sons, 1985.

FREJAFON, E. et al. Laser applications for atmospheric pollution monitoring. **The European Physical Journal D - Atomic, Molecular, Optical and Plasma Physics**, v. 4, n. 2, p. 231-238, 1998.

GUERREO-RASCADO, J. L. Multispectral elastic scanning lidar for industrial flare research: characterizing the electronic subsystem and application. **Optics Express**, v. 22, p. 31063-31077, 2014. https://doi.org/10.1364/OE.22.031063

INABA, H. Detection of atoms and molecules by raman scattering and resonance fluorescence. **Part of the Topics in Applied Physics book series,** v. 14, p.153-236, 2005. https://doi.org/10.1007/3-540-07743-X_19

KAVITA, M.; PRABHA, R.N. Non-homogeneous vertical distribution of methane over Indian region using surface, aircraft and satellite based data. **Atmospheric Environment**, v. 141, p. 174-185, 2016. https://doi.org/10.1016/j.atmosenv.2016.06.068

LEHMANN, K. K. The superposition principle and cavity ring-down spectroscopy. **Journal of chemistry and physics**, v. 105, p. 102- 63, 1996. https://doi.org/10.1063/1.472955

PAINEL INTERGOVERNAMENTAL SOBRE MUDANÇAS CLIMÁTICAS (IPCC). **AR5**. Disponible in: https://archive.ipcc.ch/pdf/assessment-report/ar5/syr/SYR_AR5_FINAL_full_wcover.pdf. Acess in: June, 2020.

RAHIMPOUR, M. R.; JAMSHIDNEJAD, Z.; JOKAR, S. M.; GHORBANI, A.; MOHAMMADI, A. H. A comparative study of three different methods for flare gas recovery of Asalooye Gas Refinery. **Journal of Natural Gas Science and Engineering.** v. 4, p.17-28, 2012. https://doi.org/10.1016/j.jngse.2011.10.001

VESELOVSKII, I; GOLOUB, P; HU, O.; PODVIN, T; WHITEMAN, D. N.; KORENSKIY, M.; LANDULFO, E. Profiling of CH4 background mixing ratio in the lower troposphere with Raman lidar: a feasibility experiment. **Atmospheric Measurements Techniques Discuss**, v. 12, p. 119-128, 2019. https://doi.org/10.5194/amt-12-119-2019

WEBER, A. **High-resolution rotational raman spectra of gases**. New York: Springer, 1979. https://doi.org/10.1007/978-3-642-81279-8_3

WEIBRING, P.; ANDERSSON, M.; EDNER, H.; SVANBERG, S. Remote monitoring of industrial emissions by combination of lidar and plume velocity measurements**. Appl. Phys.** B 66, p. 383–388 (1998). https://doi.org/10.1007/s003400050405

WEITKAMP, C. LIDAR **Range-resolved optical remote sensing of the atmosphere**. [S.l.]: Springer, (2005). https://doi.org/10.1007/b106786